


## ORIGINAL RESEARCH

# Enolase2 regulates seed fatty acid accumulation via mediating carbon partitioning in *Arabidopsis thaliana*

Zijin Liu<sup>1,2</sup> | Huimin Liu<sup>1</sup> | Lamei Zheng<sup>1</sup> | Fan Xu<sup>3</sup> | Yu Wu<sup>1</sup> | Li Pu<sup>3</sup> | Genfa Zhang<sup>1</sup> 

<sup>1</sup>Beijing Key Laboratory of Gene Resource and Molecular Development, College of Life Sciences, Beijing Normal University, Beijing, China

<sup>2</sup>College of Agronomy, Northwest A&F University, Yangling, Shaanxi, China

<sup>3</sup>Biotechnology Research Institute, Chinese Academy of Agriculture Sciences, Beijing, China

## Correspondence

Li Pu, Biotechnology Research Institute, Chinese Academy of Agriculture Sciences, Beijing 100081, China.  
Email: [puli@caas.cn](mailto:puli@caas.cn)

Genfa Zhang, Beijing Key Laboratory of Gene Resource and Molecular Development, College of Life Sciences, Beijing Normal University, Beijing 100875, China.  
Email: [gfzh@bnu.edu.cn](mailto:gfzh@bnu.edu.cn)

## Funding information

National Natural Science Foundation of China, Grant/Award Numbers: 31470399, 31872672

Edited by A. Marion-Poll

## Abstract

In many higher plants, fatty acid (FA) biosynthesis is coordinately regulated at multiple levels by intricate regulatory networks. However, the factors and their regulatory mechanisms underlying seed oil accumulation are still limited. Here, we identified that loss of glycolytic metalloenzyme enolase2 (*AtENO2*) activity increased the contents of total FAs and salicylic acid (SA) but reduced the accumulation of flavonoids and mucilage by regulating the expression of key genes involved in their biosynthesis pathway in *Arabidopsis thaliana* seeds. *AtENO2* physically interacts with the transcription factor *AtTGA5*, which may participate in the regulation of SA levels. Non-targeted metabolomics analysis of *eno2*<sup>-</sup> and WT also showed that the levels of three flavonoids, quercetin-3-galactoside, quercitrin, and epicatechin, were significantly decreased in *eno2*<sup>-</sup>, and the flavonoid biosynthesis pathway was also enriched in the KEGG analysis. Meanwhile, the mutation of *AtENO2* delayed silique ripening, thereby prolonging silique photosynthesis time, allowing siliques to generate more photosynthesis products for FA biosynthesis. These results reveal a molecular mechanism by *AtENO2* to regulate seed oil accumulation in *A. thaliana*, providing potential targets for improving crop seed oil quality.

## 1 | INTRODUCTION

In higher plants, fatty acids (FAs) and FA-derived complex lipids of seeds are not only the main storage form of energy and carbon sources but also one of the most important human nutrients. They facilitate seed germination and seedling establishment, and serve as feedstock for biofuel production (Rogalski & Carrer, 2011; Zhang et al., 2012; Zhou et al., 2019). In *Arabidopsis thaliana* seeds, FAs and lipids account for approximately 33–43% of the storage compounds (Xuan et al., 2018), and there are eight FA components, namely, palmitic acid (C16:0), stearic acid (C18:0), oleic acid (C18:1), linoleic acid (C18:2), linolenic acid (C18:3), arachidonic acid (C20:0), gondoic acid (C20:1), and erucic acid (C22:1). FAs are rapidly synthesized and accumulated at the 7–17 DAF (days after

flowering) stage, with the contents reaching a peak at 18 DAF (Baud & Lepiniec, 2009). To date, we have known that FA biosynthesis is affected by many factors, such as enzymes (von Wettstein-Knowles et al., 2006; Wu & Xue, 2010), transcription factors (Duan et al., 2017; Kim & Delaney, 2002), plant hormones (Chen, Du, et al., 2012; Liu et al., 1995), and the external environment (Goffman et al., 2005; Namazkar et al., 2016). However, the regulation mechanisms of FA biosynthesis are quite complex and need to be further elucidated.

Flavonoids, consisting of flavonols, anthocyanins, and proanthocyanins (PAs), are highly correlated with the seed coat color, and PAs are the end products of the flavonoid biosynthesis pathway and key compounds for the formation of seed coat color (Li et al., 2019; Liu et al., 2013). Recent research on the regulatory mechanism of flavonoid biosynthesis has mainly focused on the biosynthesis of anthocyanins and PAs, which have been described

Zijin Liu, Huimin Liu, and Lamei Zheng contributed equally to this work.

in apples (Xu et al., 2020), strawberries (Wang et al., 2020), grapes (Wei et al., 2020), maize (Liu, Yang, et al., 2018), chrysanthemums (Zhong et al., 2020), and so forth. In *A. thaliana*, flavonols and anthocyanins exist in all tissues, while PAs only accumulate in the seed coat (Xu et al., 2015). Seed coat color is regarded as the most intuitive index for distinguishing crop varieties in agricultural production and is an important trait for the crop breeding of *Brassica cruciferae*, especially for oil crops. Compared with black seeds of oilseed rape of the same genetic background, the yellow-seeded rape has the advantages of thinner testa, higher oil content and better oil quality (Meng et al., 1998; Olsson, 1960; Tang et al., 1997). It has also been reported that flavonoid deficiency is the main cause of increased FA contents in *A. thaliana* (Li et al., 2006; Wang et al., 2014; Xuan et al., 2018). Therefore, it is essential to discover key genes that regulate flavonoid biosynthesis and analyze their regulatory mechanisms, which is conducive to breeding high-yield, high-quality germplasm resources of crops and excellent varieties.

Enolase (ENO, 2-phospho-D-glycerate hydrolyase), a metalloenzyme in glycolysis, which catalyzes the dehydration of 2-phospho-D-glycerate to phosphoenolpyruvate, are widely distributed and highly conserved in vertebrates and plants (Liu, Zhang, et al., 2020). There are three *ENO* genes in *A. thaliana*: *AtENO1* (At1g74030), *AtENO2* (At2g36530, also referred to *LOS2*) (Lee et al., 2002), and *AtENO3* (At2g29560). Among them, the ENO1 and ENO2 proteins possess enolase activity, while ENO3 does not (Andriotis et al., 2010; Prabhakar et al., 2009). ENO2 is located in the cytosol and nucleus, but ENO1 and ENO3 are observed in the chloroplast and cytoplasm, respectively (Andriotis et al., 2010). *AtENO2* can be alternatively translated into enolase2 and c-Myc binding protein 1-like protein (AtMBP-1). AtMBP-1 lacks enzymatic activity and represses enolase activity (Eremina et al., 2015; Liu, Zhang, et al., 2018). Mutation of *AtENO2* causes growth and reproduction defects, such as a reduced rate of pollen germination, impaired floral organogenesis, and impaired male gametophytes (Eremina et al., 2015). Our previous research showed that *AtENO2* also affected the size and weight of seeds by adjusting cytokinin content through the ENO2-bZIP75 complex (Liu, Zheng, et al., 2020). However, the roles of *AtENO2* in FA and flavonoid biosynthesis remain largely unknown.

In this study, we found that the functional loss of *AtENO2* reduced the accumulation of flavonoids and mucilage while increasing the total FA via mediating carbon partitioning in *A. thaliana* seeds. The ripening delay of siliques due to the *AtENO2* mutation would prolong silique photosynthesis time, allowing siliques to generate more photosynthesis products for FA biosynthesis. In addition, *AtENO2* interacts with the transcription factor AtTGA5 and the *AtENO2*-AtTGA5 complex may involve in the regulation of salicylic acid (SA) levels, which in turn controls FA accumulation in *A. thaliana* seed. These results reveal the novel function of *AtENO2* in the complex networks of seed FA biosynthesis and provide a promising target gene for the increase in FA content and the improvement of oil quality in crops.

## 2 | MATERIALS AND METHODS

### 2.1 | Plant materials and growth conditions

*A. thaliana* Columbia (Col-0) was used as the WT control. The *AtENO2/AtLOS2* T-DNA insertion mutants (*los2-2*, SALK\_021737; *los2-3*, SALK\_077784; *los2-4*, SAIL\_208\_B09) in the WT background were obtained from the Arabidopsis Biological Resource Center. The details of the mutation have been described by Eremina et al. (2015). Because *los2-3* and *los2-4* suffer from embryo lethality and produce no seeds, we used the mutant *los2-2* (called *eno2<sup>-</sup>* in our study) for subsequent research. The *eno2<sup>-</sup>/35S:AtENO2* line was generated in our laboratory. The recombinant plasmid containing *AtENO2* driven by the CaMV35S (35S) promoter was transformed into *eno2<sup>-</sup>* background using the floral dip method to generate *eno2<sup>-</sup>/35S:AtENO2* plants. The pretreatment of seeds for sowing and plant growth conditions were previously described in Liu, Zheng, et al. (2020).

### 2.2 | Morphological observations of mature seeds

The seeds for microscopic observations were randomly selected and photographed using a microscope manufactured by Carl Zeiss Microscopy GmbH. The oil bodies were observed under transmission electron microscopy (TEM, Hitachi, HT7800). The main steps were performed following the description by Chen et al. with slight modification (Chen, Wang, et al., 2012). Ten mature seeds of each genotype were randomly selected for sectioning. Seeds were fixed with 2.5% glutaraldehyde in phosphate buffer (0.1 M, pH 7.0) overnight at 4°C and then washed three times in phosphate buffer (0.1 M, pH 7.0) for 15 min. The seeds were then fixed with 1% osmium acid in phosphate buffer (0.1 M, pH 7.0) for 1–2 h and rinsed three times with phosphate buffer (0.1 M, pH 7.0) for 15 min, respectively. The samples were dehydrated by gradient concentrations of ethanol (50, 70, 90%) for 15–20 min each time and then transferred to a mixture of 90% ethanol:90% acetone (1:1) and 90% acetone for 15–20 min at 4°C. The specimen was placed in a 2:1 mixture of absolute acetone and the final Spur resin mixture for 3–4 h at room temperature and then transferred to a 1:2 mixture of absolute acetone and the final Spur resin mixture overnight and then to the final Spur resin mixture for 2–3 h. The embedded samples were placed in an oven at 37°C overnight and heated at 45°C for 12 h and at 60°C for 48 h. The samples were then sliced using an ultrathin microtome. After staining in 2% uranyl acetate and alkaline lead citrate for 20 min, the obtained slices were observed and photographed under a transmission electron microscope.

### 2.3 | Vanillin assay and ruthenium red staining

The vanillin assay and ruthenium red staining were carried out as described by Wang et al. (2014). Three hundred mature seeds were incubated in a solution containing 1% w/v vanillin and 6 M HCl for

1 h at room temperature. The 300 mature seeds were soaked in water for 1 h and stained using 0.01% ruthenium red solution for 2 h. The stained seeds were observed and photographed using a microscope manufactured by Carl Zeiss Microscopy GmbH.

## 2.4 | Measurement of flavonoid, PA, starch, and glucose contents

The contents of flavonoids and PA in 0.1 g mature and dry seeds were measured on a multiscan microplate reader (SpectraMax Plus 384) using flavonoid and PA kits (Solarbio Life Sciences). The levels of starch and glucose in siliques were measured by a Multiskan microplate reader (SpectraMax Plus 384) according to the instructions of the starch/glucose assay kit (Solarbio Life Sciences). Siliques (0.1 g) (9 DAF and 14 DAF) were randomly selected from six individual plants grown in different pots. Three biological replicates and three technical replicates were employed for each experiment.

## 2.5 | Measurement of FA content

The extraction and analysis of FAs were performed as follows (Chen, Wang, et al., 2012). Seeds (approximately 10 mg) were heated at 80°C for 2 h in 4 ml 2.5% (v/v) HCl-methanol solution containing 25  $\mu\text{g mL}^{-1}$  methyl heptadecanoate used as an internal standard. After cooling to room temperature, the FA methyl esters were extracted with 2 ml 0.9% (w/v) NaCl and 2 ml hexane and then shaken for 2 min, a process that was repeated three times. The samples were centrifuged at 2300 rpm for 5 min, and the upper organic phase was used for analysis by gas chromatography (GC). The chromatographic column (DB-5MS) was 30 m (length)  $\times$  0.5  $\mu\text{m}$  (liquid membrane thickness)  $\times$  0.25 mm (inner diameter). The initial temperature of the column was maintained at 160°C for 1 min and then increased to 240°C at a rate of 4°C  $\text{min}^{-1}$ . After running for 16 min at the final temperature, the FA species were identified by their retention times. The FA concentrations of each sample were normalized against the internal standard.

## 2.6 | Measurement of SA content

To test whether *AtENO2* affects the accumulation of SA during silique maturation, we measured the total SA in 9 DAF and 14 DAF Arabidopsis siliques of WT and *eno2<sup>-</sup>* plants using high-performance liquid chromatography (HPLC) by Suzhou Comin Biotechnology Co. Ltd., China. The machine (Agilent 1100, USA) was equipped with a Kromasil C18 reversed-phase chromatography column (250 mm  $\times$  4.6 mm, 5  $\mu\text{m}$ ), with Phase A (0.1% v/v acetic acid-phosphoric acid): Phase B (methanol (chromatographically pure)) = 4:6; injection volume: 10  $\mu\text{l}$ ; flow rate: 0.8 ml  $\text{min}^{-1}$ ; column temperature: 35°C; sampling time: 40 min. The excitation wavelength of the fluorescence detector was 294 nm, and the emission wavelength was 426 nm. The content of SA was calculated according to the standard curve.

## 2.7 | Identification and analysis of metabolites

The metabolites were extracted and identified by Lipidall Technologies. The metabolites were extracted from 7-week-old plants (roots were removed) as described previously (Yilmaz et al., 2016). Five independent biological replicates were employed. Chromatographic separation was performed on reversed-phase ACQUITY UPLC HSS T3 1.8  $\mu\text{m}$ , 2.1  $\times$  100 mm columns (Waters) using an ultra-performance LC system (Agilent 1290 Infinity II; Agilent Technologies). MS was performed using high-resolution mass spectrometry (MS; 5600 Triple TOF Plus, Applied Biosystems/MDS Sciex) equipped with an ESI source. Data were acquired in positive and negative ion modes. Metabolite identification was compared with standard references and the open-source databases HMDB (<http://www.hmdb.ca/>) and METLIN ([https://metlin.scripps.edu/landing\\_page.php?pgcontent=mainPage](https://metlin.scripps.edu/landing_page.php?pgcontent=mainPage)). Principal component analysis and orthogonal partial least square discriminant analysis (OPLS-DA) were performed using Analyst 1.6.1 software. Differentially accumulated metabolites (DAMs) were selected according to a variable importance in projection (VIP) score and  $P < 0.05$ . The enrichment analysis of DAM sets was carried out using the *Arabidopsis* metabolic pathway database (ARACYC 16.0, <https://www.plantcyc.org/databases/aracyc/16.0>).

## 2.8 | Quantitative RT-qPCR analysis

Total RNA was extracted from siliques or developing seeds by an Eastep Super Total RNA Extraction Kit (Promega) and then reverse-transcribed into cDNA by the GoScript™ Reverse Transcription System (Promega). RT-qPCR was performed to detect the transcript levels of genes using TransStart Top Green qPCR SuperMix (TransGen Biotech). Arabidopsis *EF1aA4* was used as the internal control to normalize the relative transcriptional abundance, and the control sample was conferred a value of 1. The primers are listed in Table S1.

## 2.9 | Yeast two-hybrid assay

The coding sequences (CDSs) of *AtENO2* and *AtMBP-1* were amplified by PCR as described previously (Kang et al., 2013) and then cloned into pGBKT7. The CDS of TGACG motif-binding factor 5 (TGA5) was cloned into pGADT7 using gene-specific primers (Table S1). The yeast two-hybrid (Y2H) gold yeast strain harboring these recombinant plasmids was cultured on media lacking Trp/Leu, Trp/Leu/His, or Trp/Leu/His/Ade.

## 2.10 | Pull-down assay

The CDS of TGA5 was inserted into pET-28a with a His-tag, and the CDSs of *ENO2* and *MBP-1* were cloned into the GST-tagged

pGEX-6P-1 vector. The TGA-5-His, ENO2-GST, and MBP-1-GST fusion proteins were induced with IPTG (isopropyl β-D-1-thiogalactopyranoside) at 16°C for 12–14 h after transforming the recombinant plasmids into *Escherichia coli* BL21. The proteins were purified according to the manufacturer's instructions (Beyotime Biotechnology), and then the mixture of purified ENO2-GST/MBP-1-GST protein and TGA-5-His protein was incubated with GST-tagged bait protein and rotated at 4°C for 8–12 h. After washing three times with PBS buffer, the fusion proteins were eluted by elution buffer and detected by western blotting using His and GST antibodies, respectively. The primers used are shown in Table S1.

## 2.11 | Luciferase complementation imaging assays

Luciferase complementation imaging (LUC) assays were performed as described by Liu, Zheng, et al. (2020a). The pairs of *Agrobacterium tumefaciens* strain GV3101 harboring ENO2-nLuc + cLuc-TGA5, MBP-1-nLuc + cLuc-TGA5, ENO2-nLuc + cLuc, MBP-1-nLuc + cLuc, nLuc + cLuc-TGA5, and nLuc + cLuc were transformed into *Nicotiana benthamiana* leaves. After expression for 48 h, the leaves were treated with luciferin, and the signal was detected by CCD. The primers used for generating the fusion constructs are listed in Table S1.

## 2.12 | Bimolecular fluorescence complementation assays

Bimolecular fluorescence complementation (BiFC) assays were carried out as described by Liu, Zheng, et al. (2020). The CDSs of ENO2 and MBP-1 were cloned into pSYNE, while that of TGA5 was cloned into pSYCE. The primers for these constructs are listed in Table S1. The plasmids were transformed into *A. tumefaciens*, which was then infiltrated into *N. benthamiana* leaves. Leaves were observed 2 days after infiltration under a confocal microscope (Zeiss LSM 880).

## 2.13 | Statistical analysis

Figures were prepared, and statistical analysis was performed by GraphPad Prism 8.0 software. Differences between groups were evaluated by significant difference analysis (Student's *t* test,  $P \leq 0.05$ ). Data are expressed as the means  $\pm$  sd.

# 3 | RESULTS

## 3.1 | AtENO2 positively regulates the biosynthesis of mucilage and flavonoids

To characterize the function of *AtENO2* during seed development, we first confirmed the *AtENO2* mutant (*eno2*<sup>-</sup>) was homozygous by

genotyping (Figure S1A). The expression level of *AtENO2* was examined by RT-qPCR, and the results showed that it was significantly reduced in *eno2*<sup>-</sup> compared to WT and *eno2*<sup>-</sup>/*35S:AtENO2* (Figure S1B). Western blot assays further validated that the ENO2 and MBP-1 proteins which were alternatively translated from *AtENO2* mRNA, were detected in WT and *eno2*<sup>-</sup>/*35S:AtENO2* but not in *eno2*<sup>-</sup> (Figure S1C). The representative *eno2*<sup>-</sup> and *eno2*<sup>-</sup>/*35S:AtENO2* lines, as well as WT plants, were selected for further experiments. As shown in Figure 1A, we found that the seed coat color of *eno2*<sup>-</sup> was lighter than those of WT and *eno2*<sup>-</sup>/*35S:AtENO2* seeds, which both showed brown. It has been reported that PA, a flavonoid, is the main type of pigment deposited in the seed coat of *A. thaliana* (Debeaujon et al., 2001). We then performed the vanillin assay to test PA deposition and found that the PA staining of *eno2*<sup>-</sup> seed coats was lighter than those of WT and *eno2*<sup>-</sup>/*35S:AtENO2*, which is consistent with the lighter seed color observed in mutants, suggesting that PA deposition was reduced in the *eno2*<sup>-</sup> seed coat (Figure 1B). In accordance with PA staining results, the quantitative measurement of PA confirmed that *AtENO2* mutation decreased the seed PA content (Figure 1C). Simultaneously, the total flavonoid content was significantly lower than that of WT (Figure 1D). The results of ruthenium red staining also showed that the mucilage layers in the *eno2*<sup>-</sup> were thinner than those of the corresponding WT in terms of thickness (Figure 1E). These results suggested that the mutation of *AtENO2* inhibits the biosynthesis of mucilage and flavonoids, especially PA, which results in a yellow seed coat.

## 3.2 | AtENO2 negatively regulates seeds oil accumulation

Given that flavonoid deficiency is the main cause of increased FA contents (Xuan et al., 2018), we measured the total FA contents in WT, *eno2*<sup>-</sup> and *eno2*<sup>-</sup>/*35S:AtENO2* seeds by using GC-MS analysis. The results showed that the contents of C18:1, C18:2, C18:3, C20:1, and C22:1 in the *eno2*<sup>-</sup> seeds were significantly higher than those in WT and *eno2*<sup>-</sup>/*35S:AtENO2* seeds (Figure 2A), accompanied by the increase of total seed FA level in *eno2*<sup>-</sup> seeds (Figure 2B). The larger oil bodies were also observed in *eno2*<sup>-</sup> seeds than in WT (Figure 2C,D). These results suggested that *AtENO2* negatively regulates oil accumulation in *A. thaliana* seeds.

## 3.3 | AtENO2 regulates the expression of key genes contributing to FA biosynthesis

To further reveal the possible mechanism by which *AtENO2* affects the seed FA content, we conducted RT-qPCR to detect the expression patterns of several key genes involved in FA biosynthesis in WT and *eno2*<sup>-</sup> developing seeds. As shown in Figure 3, the expression levels of *ENOLASE1* (*ENO1*, AT1G74030), *BIOTIN CARBOXYL CARRIER PROTEIN2* (*BCCP2*, AT5G15530), *FATTY ACID*

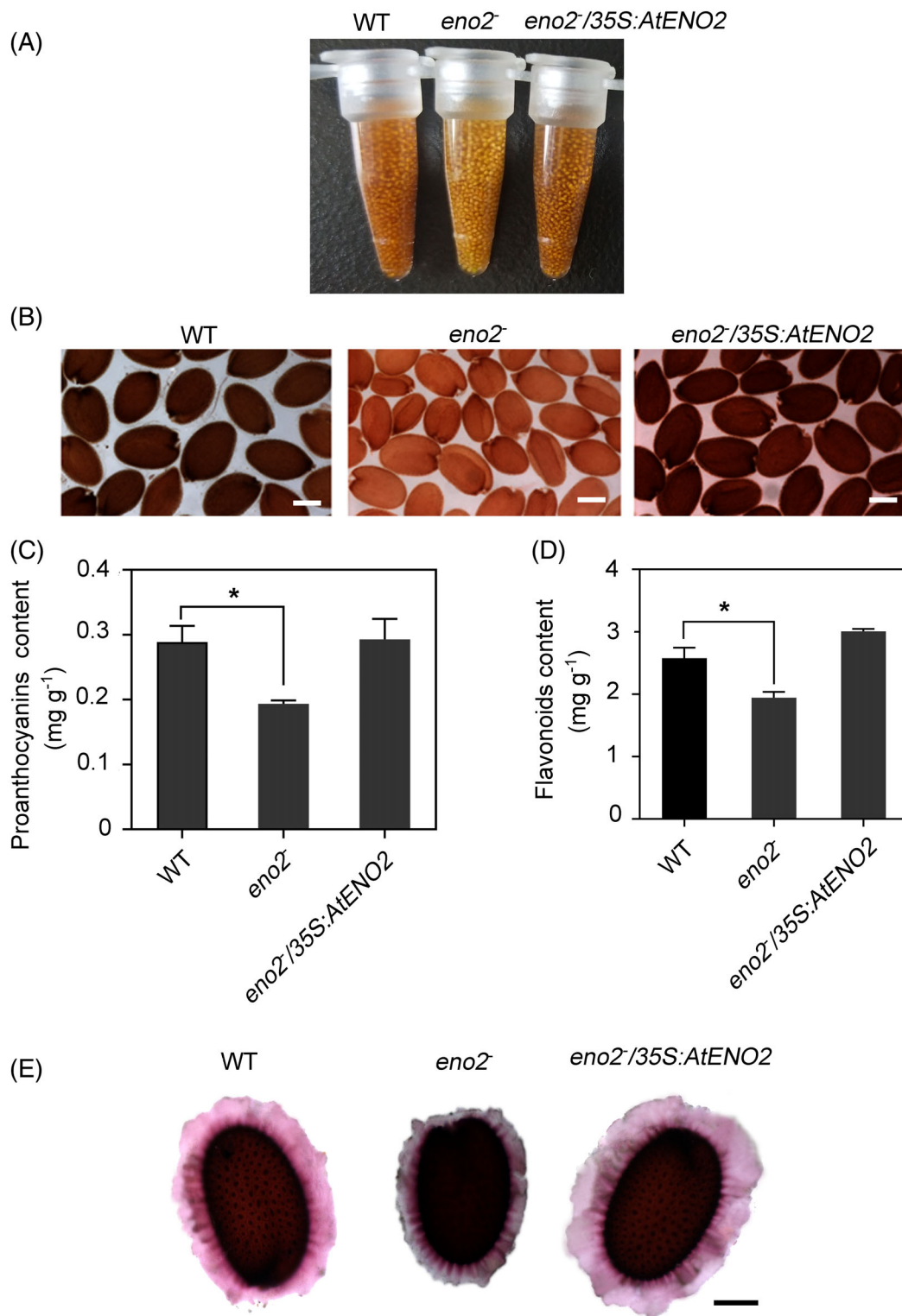


**FIGURE 1** Characterization of *AtENO2* function in seed flavonoid and mucilage biosynthesis. (A) The seed coat color, (B) the seeds of the group soaked in vanillin-HCl solution, (C) the content of proanthocyanins, and (D) the content of total flavonoids. Bar: 200  $\mu$ m. (E) The mucilage layer attached to the seed coat among WT, *eno2*<sup>-</sup> and *eno2*<sup>-</sup>/*35S:AtENO2* seeds. Bar: 100  $\mu$ m

DESATURASE2 (*FAD2*, AT3G12120), *FAD3* (AT2G29980), *FATTY ACID ELONGASE 1* (*FAE1*, At4g34520), and *DIACYLGLYCEROL ACYLTRANSFERASE2* (*DGAT2*, AT3G51520) were significantly higher in

*eno2*<sup>-</sup> than in the WT (Figure 3). These results indicate that the mutation of *AtENO2* promotes the expression of genes contributing to FA accumulation.



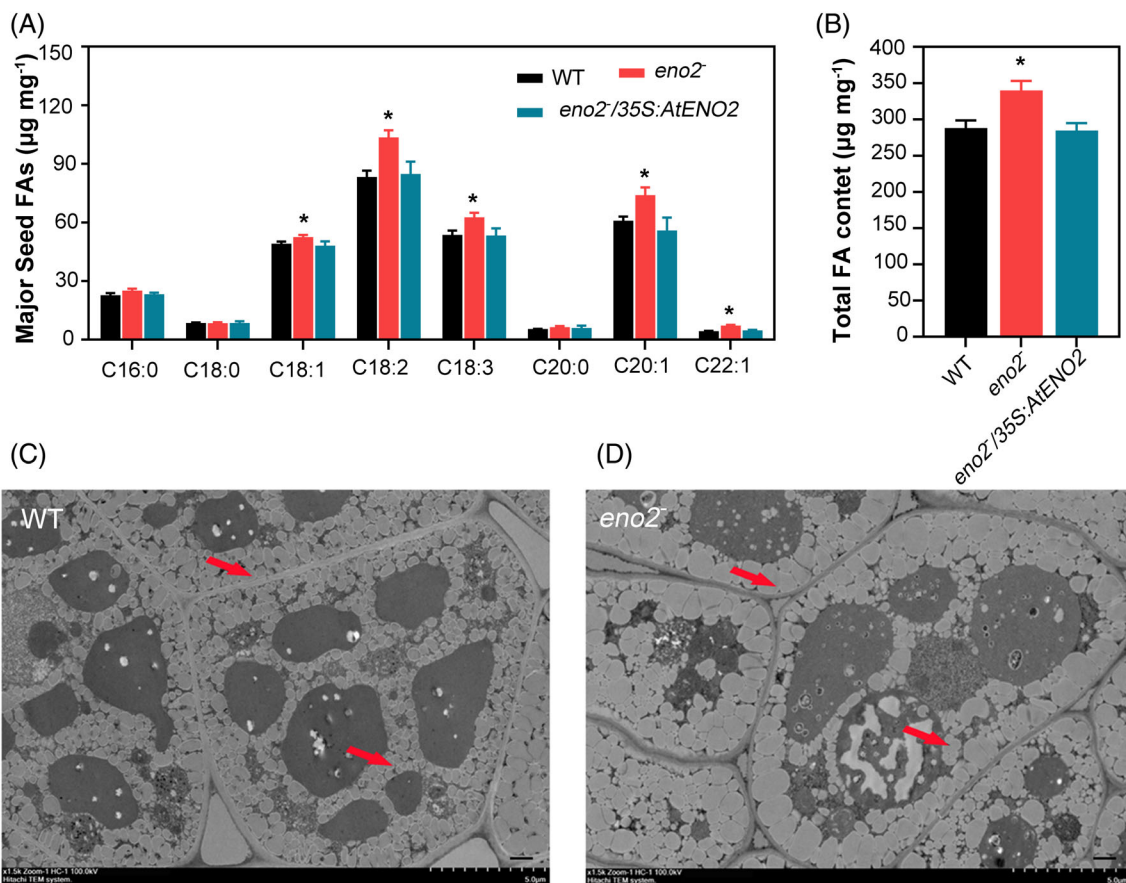


**FIGURE 2** Characterization of AtENO2 in the accumulation of seed FAs. (A) and (B) represent the contents of FA composition and total FAs in different genotypes, respectively. (C) and (D) represent the subcellular differences in WT and *eno2*<sup>-</sup>, respectively. The red arrows represent oil bodies in WT and *eno2*<sup>-</sup> seeds.

### 3.4 | Metabolic features of differentially accumulated metabolites in WT and *eno2*<sup>-</sup>

To systematically profile metabolic changes in WT and *eno2*<sup>-</sup>, we conducted a non-targeted metabolite analysis. The total variation was divided into two major components by principal component analysis, which contributed 33.2 and 22.6%, respectively (Figure 4A). The correlation coefficients of five samples in the WT and *eno2*<sup>-</sup> groups were close to 1 (Figure S2A), and WT and *eno2*<sup>-</sup> samples were classified into two categories (Figure S2B). These results indicated that the sample repeatability and the results of metabolite analysis are reliable. We then performed OPLS-DA to obtain a higher level of group separation. The high predictability ( $Q^2Y = 92.4\%$ ) of the OPLS-DA models was observed, and 64.2% ( $R^2X$ ) of the variables were able to explain the 99.7% ( $R^2Y$ ) difference in the comparison of WT and *eno2*<sup>-</sup> (Figure 4B).

We detected a total of 126 metabolites (Table S2), of which 27 were defined as differentially accumulated metabolites (DAMs) that exhibited a VIP > 1 and  $P$ -value < 0.05 (Table S3). There were 10 upregulated DAMs and 17 downregulated DAMs. The metabolites covered two major categories and included 8 amino acids and 4 flavonoid glycosides (Figure 4C). The accumulation profiles

showed that the levels of quercetin-3-galactoside, quercitrin, and epicatechin, which belong to flavonoids, were significantly decreased in *eno2*<sup>-</sup> (Figure 4D). Consistent with this, we found that the flavonoid biosynthesis pathway was also enriched in the KEGG analysis (Figure 4E). To identify the regulatory network of AtENO2 in *A. thaliana*, we constructed the key metabolic pathways regulated by AtENO2 based on metabolomic analysis. As shown in Figure 4F, the loss of AtENO2 mainly affected the tricarboxylic acid cycle, flavonoid and amino acid synthesis. Among them, the metabolite contents involved in the tricarboxylic acid cycle and flavonoid synthesis pathways in *eno2*<sup>-</sup> were all lower than those in WT, while the contents of metabolites related to amino acid synthesis in *eno2*<sup>-</sup> were higher than those in WT.

### 3.5 | AtENO2 interacts with the transcription factor AtTGA5

To gain insight into the function of AtENO2 in *A. thaliana*, we identified the interacting proteins with AtENO2 and AtMBP-1 using ENO2/MBP-1 as a bait for screening libraries of *A. thaliana* cDNAs. We first generated a sequence that only expresses the AtENO2 protein and

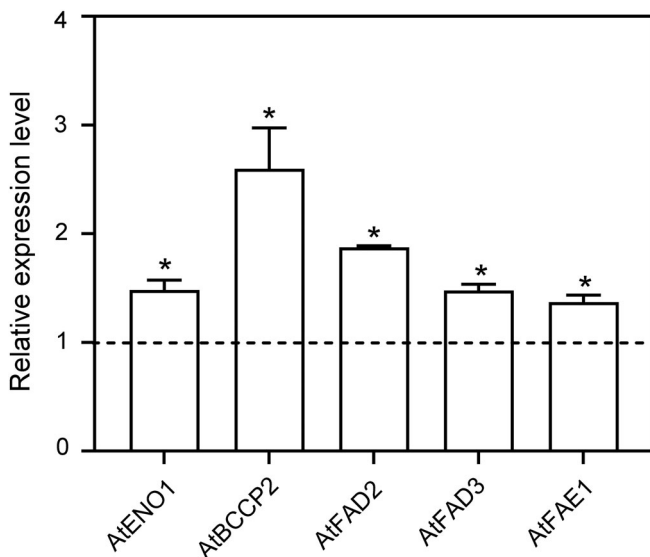


**FIGURE 3** Comparison of the expression of genes involved in fatty acid accumulation in the 12 days after flowering (DAF) developing seeds of the wild type and *eno2*<sup>-</sup>. The results were normalized against the expression of *AtEF1aA4* as an internal control, and the expression level of each examined gene in the wild type was set to 1.0. Values are the mean  $\pm$  SD ( $n = 3$ ). Asterisks indicate significant differences in gene expression levels in *eno2*<sup>-</sup> plants compared with those in wild-type plants (two-tailed paired Student's *t* test,  $P \leq 0.05$ ). Error bars denote SD.

that only expresses the AtMBP-1 protein from *A. thaliana*, according to Kang et al. (2013). Then, the Y2H results showed that yeast cells were grown in the selection medium only when ENO2-BD/MBP-1-BD and TGA5-AD were co-transformed (Figure 5A), indicating that both AtENO2 and AtMBP-1 may interact with AtTGA5. To obtain additional evidence for the interaction of ENO2/MBP-1 and TGA5, we performed in vitro pull-down analysis. Both the GST-TGA5, His-ENO2 and His-MBP-1 recombinant proteins were produced and purified. In the following in vitro binding assay, GST-TGA5 specifically bound His-ENO2 but not His-MBP-1 or GST (Figure 5B). Therefore, TGA5 and ENO2 directly interact in vitro.

To further verify whether the in vitro interaction of ENO2 with TGA5 could be recapitulated specifically in vivo, we performed a luciferase complementation (LUC) assay and a BiFC assay. The LUC assay showed that the luciferase activity was detected in *N. benthamiana* leaves co-transformed with ENO2-nLUC and cLUC-TGA5 constructs, whereas the negative control and/or MBP-1-nLUC + cLUC-TGA5 did not have luciferase activity, indicating that AtENO2 associates with AtTGA5 in vivo (Figure 5C). Furthermore, the YFP fluorescence signal was observed in cells co-expressing TGA5-cYFP with ENO2-nYFP but not MBP-1-nYFP, and the TGA5/Eno2 complex localized to the nucleus. The fluorescence signal was not detected in cells co-expressing TGA5-cYFP with MBP-1-nYFP (Figure 5D), which provided further proof of a specific ENO2-TGA5 interaction. Collectively, these results indicated that AtENO2 interacts with AtTGA5.

### 3.6 | AtENO2 negatively regulates the accumulation of SA

TGA5 belongs to class II of basic region/leucine zipper motif (bZIP) transcription factors. Given that class II TGA proteins act as regulatory components of the SA signaling pathway, which mediates the signaling network of jasmonic acid/ethylene, and regulates the biosynthesis of secondary metabolites (Lv et al., 2019; Pu et al., 2009; Van der Does et al., 2013; Zander et al., 2010), the effect of AtENO2 on the biosynthesis of SA was investigated. Interestingly, we found that the relative expression pattern of TGA5 in 9 DAF and 14 DAF *eno2*<sup>-</sup> siliques was significantly lower than those in WT siliques (Figure 6A). Besides, the key genes involved in the SA biosynthetic pathway, such as ENHANCED PSEUDOMONAS SUSCEPTIBILITY 1 (*EPS1*, AT5g67160), ISOCORISMATE SYNTHASE 1 (*ICS1*, AT1g74710) and AVRPPHB SUSCEPTIBLE 3 (*PBS3*, AT5g13320) were significant upregulated at 9 DAF and 14 DAF in *eno2*<sup>-</sup> siliques compared with those in WT siliques (Figure 6B–D). Consistently, the SA content was increased by the mutation of *AtENO2* at 9 DAF and 14 DAF siliques (Figure 6E). These results suggested that *AtENO2* negatively regulates the accumulation of SA in the developing siliques from *A. thaliana*.

### 3.7 | AtENO2 affects glucose and starch accumulation in siliques

It has been shown that SA delays the ripening of fruits and changes the contents of bioactive compounds (Srivastava & Dwivedi, 2000; Valero et al., 2011). The phenomenon that *AtENO2* mutation delays the maturation of siliques has been proposed in our previous research (Liu, Zheng, et al., 2020). Therefore, we supposed that the increase of FA content in *eno2*<sup>-</sup> seeds might result from the increase in carbon source required for FA synthesis, which is caused by the delay of silique ripening and the increase of photosynthesis time. To confirm our hypothesis, we measured the contents of glucose and starch in 9 DAF and 14 DAF siliques from WT, *eno2*<sup>-</sup> and *eno2*<sup>-</sup>/*35S:AtENO2*. As shown in Figure 7, the contents of glucose and starch were uniformly increased by the mutation of *AtENO2* relative to WT (Figure 7B,C). These results indicated that the mutation of *AtENO2* indeed accumulated more photosynthetic products in siliques by delaying their ripening.

## 4 | DISCUSSION

Previous studies showed that yellow seed is a desirable trait for oil-seed rape crop breeding because it has a thinner seed coat, a reduced percentage of pigment and hull, and a greater content of oil and proteins than the black-seeded type (Heneen et al., 2012; Meng et al., 1998; Tang et al., 1997; Zhai et al., 2019). The *A. thaliana* and oilseed rape belong to the closely related Cruciferous plants and accumulating evidence demonstrates that their homologous genes have similar functions on the regulation of growth and development

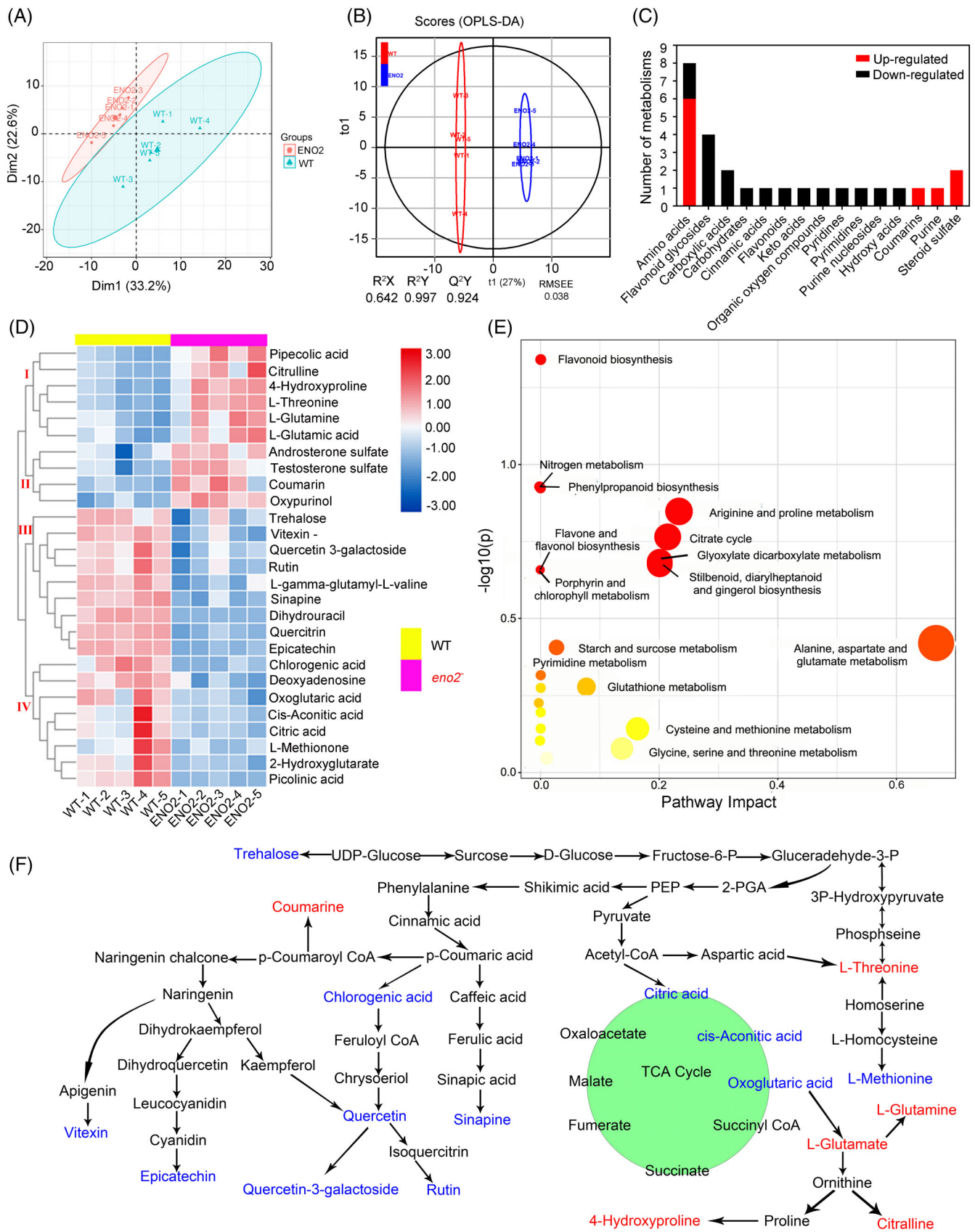
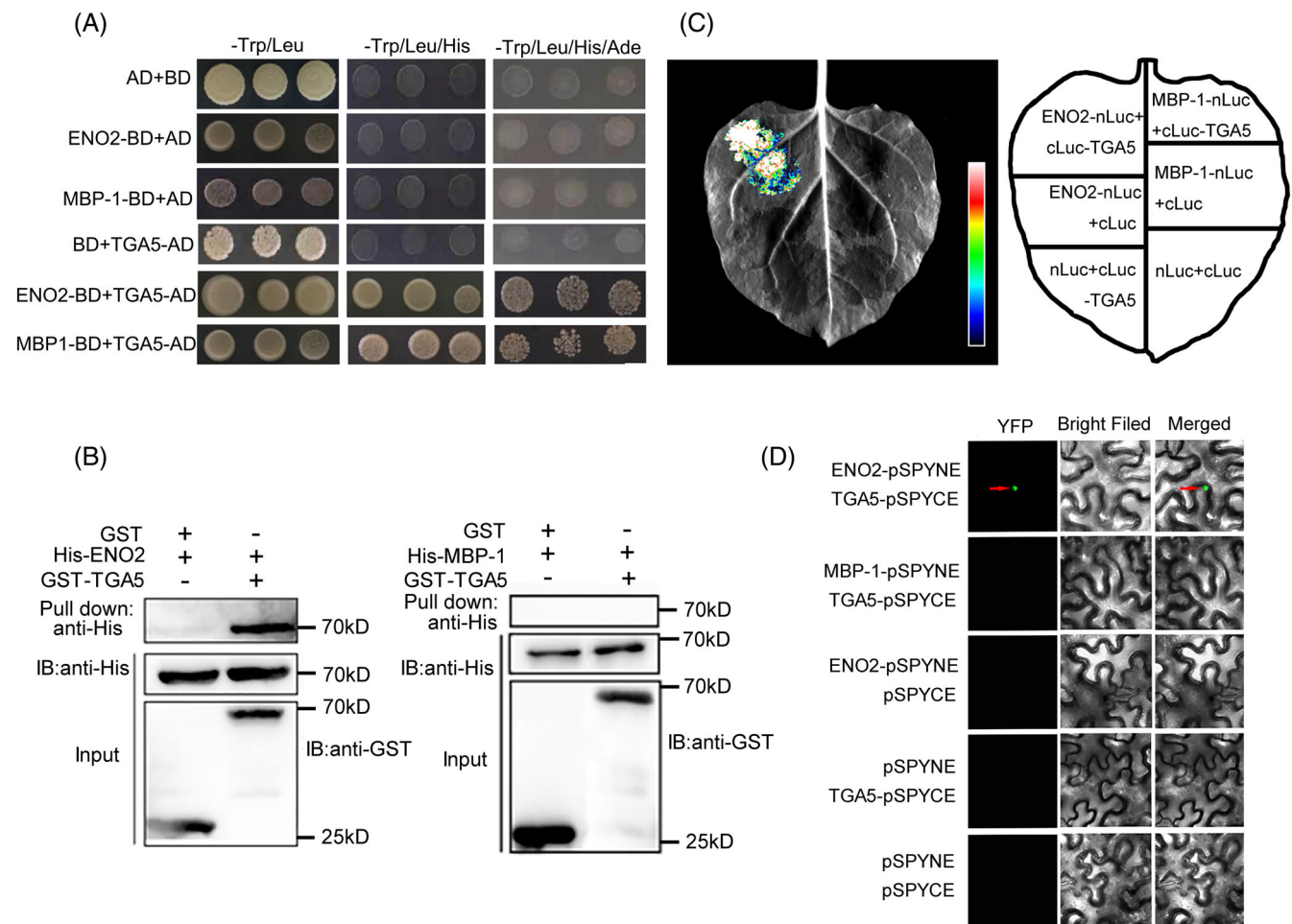


FIGURE 4 Legend on next page.





**FIGURE 5** AtENO2, but not AtMBP-1, interacts with AtTGA5 in vitro and in vivo. (A) Yeast two-hybrid assay demonstrating the interaction between AtENO2 and AtTGA5 and AtMBP-1 and AtTGA5. ENO2-BD, MBP-1-BD, and TGA5-AD constructs were co-transformed into golden yeast cells in pairwise combinations. The AD/BD, TGA5-AD/BD, AD/ENO2-BD, and AD/MBP-1-BD combinations were employed as negative controls. The co-transformed colonies were selected on synthetic dextrose –Trp/–Leu, –Trp/–Leu/–His, and –Trp/–Leu/–His/–Ade media. (B) Pull-down assay showing the interaction of AtTGA5 and AtENO2 but not AtMBP-1. Purified GST-TGA5 or GST proteins were immunoprecipitated with GST beads. Immunoprecipitated proteins were incubated with His-ENO2 or His-MBP-1. The interactions were detected by immunoblotting with an anti-His antibody. (C) Luciferase complementation imaging (LUC) assays revealing that only AtENO2 interacts with AtTGA5. ENO2-nLuc/cLuc-TGA5, MBP-1-nLuc/cLuc-TGA5, ENO2-nLuc/cLuc, nLuc/cLuc, nLuc/cLuc-TGA5, and nLuc/cLuc were co-transformed into *Nicotiana benthamiana* leaves and tested after 48 h. The pseudocolor bar represents the range of luminescence intensity in the image. (D) Bimolecular fluorescence complementation (BiFC) assays revealing the interaction of AtTGA5 and AtENO2 instead of AtMBP-1. The construct combinations were co-transformed into *N. benthamiana* leaves and expressed for 48 h. The interaction signal was detected by confocal microscopy under 60 $\times$  magnification.

(Aguilar et al., 1996; Lu et al., 2019; Martín et al., 1997). Therefore, the functional studies of genes from *A. thaliana* are helpful to elucidate the functions of homologous genes from oilseed rape. In this study, we observed that the seed coat color of *eno2*<sup>-</sup> was more yellow than the WT (Figure 1A). Consistently, the levels of flavonoids,

especially PA, which confer on seeds a dark color by their oxidation during maturation, were relatively low in *eno2*<sup>-</sup> seeds (Figure 1C). Metabolomics analysis revealed that the accumulations of quercetin-3-galactoside, quercitrin, and epicatechin, annotated as part of flavonoid metabolism, were also strongly reduced in *eno2*<sup>-</sup> plants

**FIGURE 4** Metabolite profiles of WT and *eno2*<sup>-</sup>. (A) Principal component analysis (PCA), (B) orthogonal and partial least squares-discriminate analysis (OPLS-DA), and (C) the classification of differentially accumulated metabolites (DAMs). DAMs were screened based on variable importance in project (VIP) score >1 and  $P \leq 0.05$ . (D) The clustering analysis of DAMs, (E) KEGG pathway enrichment analysis of DAMs, and (F) schematic diagram of key metabolic pathways regulated by AtENO2 and changes in metabolite content. Red and blue indicate that the content of a particular metabolite in *eno2*<sup>-</sup> is significantly increased and decreased compared with the WT, respectively.

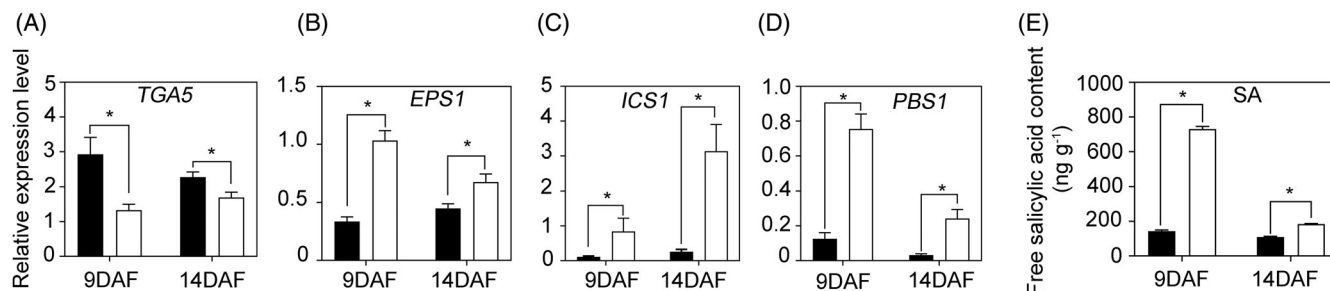


**FIGURE 6** Effect of *AtENO2* on salicylic acid (SA) biosynthesis. (A) Expression levels of *TGA5*. (B–D) Expression levels of key genes contributing to SA biosynthesis. (E) Comparison of free SA content. RNA and free SA were extracted from 9 DAF and 14 DAF siliques of wild type and *eno2*<sup>-</sup>. DAF: days after flowering. The results were normalized against the expression of *EF1aA4* as an internal control. Values are presented as the mean ± SD ( $n = 3$ ). Black and white square columns represent the wild type and *eno2*<sup>-</sup>, respectively. Asterisks indicate significant differences in gene expression levels and SA content in *eno2*<sup>-</sup> siliques compared with those in wild-type siliques (two-tailed paired Student's *t* test,  $P \leq 0.05$ ). Error bars denote SD.

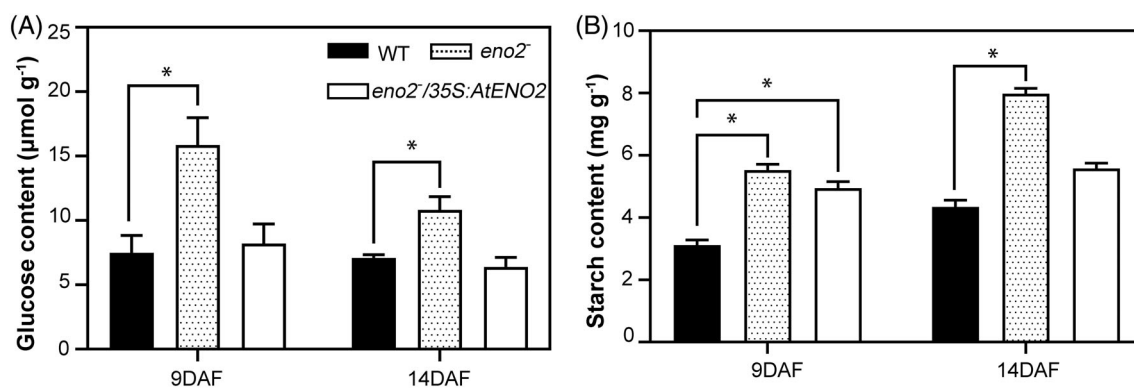


**FIGURE 7** Content comparison of glucose (A) and starch (B) between wild type, *eno2*<sup>-</sup> and *eno2*<sup>-</sup>/*35S:AtENO2* siliques. DAF: days after flowering. Asterisks indicate significant differences in *eno2*<sup>-</sup> siliques compared with those in wild-type siliques (two-tailed paired Student's *t* test,  $P \leq 0.05$ ). Error bars denote SD.

(Figure 4). The mutation of *AtENO2* also significantly reduced mucilage levels (Figure 1E). These results suggested that *AtENO2* positively regulates the flavonoid and mucilage biosynthesis in *A. thaliana* seeds.

Extensive studies have also proven that the lack of flavonoids leads to an increase in seed FA contents (Lian et al., 2017; Xuan et al., 2018). Seed FA and seed coat mucilage are also thought to be competing sinks for the limited amount of photosynthates imported into seeds, and some mucilage-deficient mutants exhibit increased seed FA levels compared with those of WT plants (Li et al., 2006; Shi et al., 2019; Wang et al., 2014). Our results also showed that *AtENO2* mutant produced seeds with elevated seed oil (Figure 2A) and larger oil bodies in mature *eno2*<sup>-</sup> seeds were observed (Figure 2C). The coordinated expression of genes involved in FA biosynthesis is essential for seed oil accumulation. *AtENO1* encodes the plastid-localized enolase that functions metabolically in the conversion of glyceraldehyde-2-phosphate into phosphoenolpyruvate, which mediates the production of acetyl-CoA, the precursor for FA biosynthesis (Prabhakar et al., 2009). The carboxylation of acetyl-CoA catalyzed by heteromeric acetyl-CoA carboxylase (HtACCCase) to yield malonyl-CoA is a primary reaction during de novo FA biosynthesis (Baud & Lepiniec, 2009). The *AtBCCP2* encodes a subunit of HtACCCase which

acts as a sensor or gating system that controls the overall flux of FA biosynthesis (Mu et al., 1998; Thelen & Ohlrogge, 2002). Therefore, the upregulated expression of *AtBCCP2* by *AtENO2* mutation should increase the overall flux of seed FAs at the early stage of the FA biosynthesis pathway. *AtFAD2* and *AtFAD3* are responsible for the biosynthesis of C18:2 and C18:3, respectively. (Puttick et al., 2009; Wang et al., 2021; Wu et al., 2010). *AtFAE1* is essential for the elongation of the FA carbon chain from C18 to C20 and C22, and possesses a high substrate specificity for 18:1-CoA (James Jr et al., 1995; Kunst et al., 1992). As a consequence of the highly upregulated expression of *AtFAD2*, *AtFAD3*, and *AtFAE1* (Figure 3), the contents of C18:2, C18:3, C20:1, and C22:1 in seeds were increased when the *AtENO2* function was lost in *A. thaliana* (Figure 2).

In addition, we confirmed that *AtENO2* interacted with *AtTGA5* (Figure 5). *AtTGA5*, a bZIP transcription factor, is responsive to SA by interacting with NPR1 (encoded by *Nonexpressor of Pathogenesis-related Gene 1*), which increases the level of SA by positively regulating the expression of SA biosynthetic genes (Kim & Delaney, 2002; Torrens-Spence et al., 2019). In order to understand the effect of *AtENO2* on SA biosynthesis, we tested the SA content in the developing siliques. The results showed that the mutation of *AtENO2*

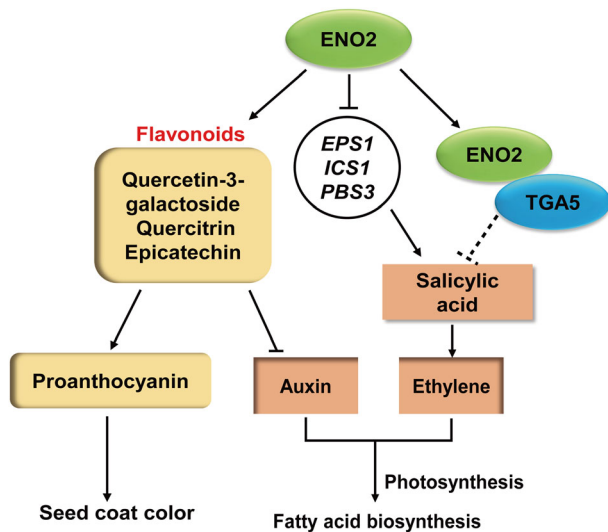


**FIGURE 8** Schematic illustrating the regulatory network for AtENO2 regarding the promotion of proanthocyanin accumulation and inhibition of fatty acid biosynthesis in seeds. Arrows indicate promoting or increasing effects, whereas blunt arrows indicate inhibiting or decreasing effects. The dotted line indicates that the specific regulatory mechanism needs to be further studied.

elevated the SA level in siliques (Figure 6E). In *A. thaliana*, SA biosynthesis mainly consists of two pathways: the cytosolic PHENYLALANINE AMMONIA LYASE pathway, which produces approximately 10% SA, and the plastid-localized ISOCHORISMATE SYNTHASE pathway, which generates approximately 90% SA (Garcion et al., 2008). RT-qPCR results showed that the key genes involved in the plastid-localized ISOCHORISMATE SYNTHASE pathway were significantly upregulated in the 9 DAF and 14 DAF siliques of *eno2*<sup>-</sup> (Figure 6). These results indicated that AtENO2 controls SA accumulation by negatively coordinating the expression of SA biosynthetic genes. Notably, SA-deficient mutants have low levels of triacylglycerol (Xu et al., 2022), and the foliar application of SA on soybean and rapeseed increases the contents of some unsaturated FAs (C18:1, C18:2, and C18:3) (Ganj-Abadi et al., 2021; Ghassemi-Golezani & Farhangi-Abzari, 2018). Thus, the AtENO2-mediated SA may also affect FA biosynthesis in *A. thaliana* seeds.

Previous studies have indicated that seed FA biosynthesis is positively regulated by auxin, and that the transport of auxin from the tip back on both sides as well as biosynthesis is inhibited by flavonoids (Buer & Muday, 2004; Xuan et al., 2018). SA delays fruit ripening by inhibiting ethylene biosynthesis (Kumar et al., 2021; Srivastava & Dwivedi, 2000). Either increased auxin level or decreased ethylene content delays fruit ripening (Barry & Giovannoni, 2007; Liu, Zhang, et al., 2020; Sravankumar et al., 2018). Our previous research also showed that the absence of ENO2 elevated the level of auxin and decreased the ethylene content in *A. thaliana* seeds (Liu, Zheng, et al., 2020). The maturity ratio of *eno2*<sup>-</sup> siliques was lower than that of WT at the same time we tested (Liu, Zheng, et al., 2020). Herein, we also found that the contents of glucose and starch produced by photosynthesis were more markedly increased at 9 DAF and 14 DAF in *eno2*<sup>-</sup> siliques

(Figure 7). Together, these results suggested that mutation of *AtENO2* causes the delay in the ripening time of siliques to produce more carbohydrates by changing the levels of auxin, ethylene, and SA. Although the glycolytic pathway in the cytoplasm is blocked because of the mutation of *AtENO2* in *eno2*<sup>-</sup> seeds, this pathway still proceeds normally in the plastid, where *AtENO1* functions in enolase activity. The mutation of *AtENO2* also upregulated the *AtENO1* expression (Figure 3). Therefore, photosynthates can be used for FA biosynthesis via the plastid-localized glycolytic pathway, which is the main pathway of FA biosynthesis.

In summary, flavonoids and SA affect the accumulation of FAs through two metabolic pathways regulated by *AtENO2* in *A. thaliana* seeds. As illustrated in Figure 8, on the one hand, the loss of *AtENO2* function in *eno2*<sup>-</sup> seeds reduced flavonoid accumulation but increased the FA content; on the other hand, the mutation of *AtENO2* causes more carbohydrates to flow into the plastid and promotes the upregulation of key genes in the plastid-localized ISOCHORISMATE SYNTHASE pathway, thereby increasing the SA level, which may also be regulated by the formation of the ENO2-TGA5 complex. Moreover, the increased SA reduces the ethylene content in *A. thaliana* seeds, which delays the maturation of siliques and prolongs the time of photosynthesis in *eno2*<sup>-</sup>. Consequently, more photosynthesis products could be produced for FA biosynthesis in *A. thaliana* seeds. How ENO2 interacts with TGA5 and the ENO2-TGA5 complex mediate the SA biosynthesis needs to be determined in the future.

#### AUTHOR CONTRIBUTIONS

Genfa Zhang, Zijin Liu, Huimin Liu and Lamei Zheng designed the study. Zijin Liu and Huimin Liu analyzed the data and drafted the manuscript. Zijin Liu and Lamei Zheng performed most of the experiments. Huimin Liu carried out the RT-qPCR. Huimin Liu drew all the graphs. Fan Xu and Yu Wu collected relative references. Genfa Zhang and Li Pu provided the experiment support. All authors read and approved the final manuscript.

#### ACKNOWLEDGMENT

We would like to thank the Experimental Technology Center for Life Science, Beijing Normal University, and we would be grateful to Jin Liu and Chao Xi for their instrument guidance.

#### CONFLICT OF INTEREST

The authors declare that there are no conflicts of interest.

#### DATA AVAILABILITY STATEMENT

All data presented are available in the article and in the supporting information.

#### ORCID

Genfa Zhang  <https://orcid.org/0000-0002-0967-4939>

#### REFERENCES

Aguilar, I., Sánchez, F., Martín, A., Martínez-Herrera, D. & Ponz, F. (1996) Nucleotide sequence of Chinese rape mosaic virus (oilseed rape

- mosaic virus), a crucifer tobamovirus infectious on *Arabidopsis thaliana*. *Plant Molecular Biology*, 30, 191–197.
- Andriotis, V.M., Kruger, N.J., Pike, M.J. & Smith, A.M. (2010) Plastidial glycolysis in developing *Arabidopsis* embryos. *The New Phytologist*, 185, 649–662.
- Barry, C.S. & Giovannoni, J.J. (2007) Ethylene and fruit ripening. *Journal of Plant Growth Regulation*, 26, 143.
- Baud, S. & Lepiniec, L. (2009) Regulation of *de novo* fatty acid synthesis in maturing oilseeds of *Arabidopsis*. *Plant Physiology and Biochemistry*, 47, 448–455.
- Buer, C.S. & Muday, G.K. (2004) The *transparent testa4* mutation prevents flavonoid synthesis and alters auxin transport and the response of *Arabidopsis* roots to gravity and light. *The Plant Cell*, 16, 1191–1205.
- Chen, M., Du, X., Zhu, Y., Wang, Z., Hua, S., Li, Z. et al. (2012) Seed fatty acid reducer acts downstream of gibberellin signalling pathway to lower seed fatty acid storage in *Arabidopsis*. *Plant, Cell & Environment*, 35, 2155–2169.
- Chen, M., Wang, Z., Zhu, Y., Li, Z., Hussain, N., Xuan, L. et al. (2012) The effect of *transparent TESTA2* on seed fatty acid biosynthesis and tolerance to environmental stresses during young seedling establishment in *Arabidopsis*. *Plant Physiology*, 160, 1023–1036.
- Duan, S., Jin, C., Li, D., Gao, C., Qi, S., Liu, K. et al. (2017) MYB76 inhibits seed fatty acid accumulation in *Arabidopsis*. *Frontiers in Plant Science*, 8, 226.
- Debeaujon, I., Peeters, A.J., Léon-Kloosterziel, K.M., & Koornneef, M. (2001) The TRANSPARENT TESTA12 gene of *Arabidopsis* encodes a multidrug secondary transporter-like protein required for flavonoid sequestration in vacuoles of the seed coat endothelium. *Plant Cell*, 13, 853–871.
- Eremina, M., Rozhon, W., Yang, S. & Poppenberger, B. (2015) ENO2 activity is required for the development and reproductive success of plants, and is feedback-repressed by AtMBP-1. *The Plant Journal*, 81, 895–906.
- Ganj-Abadi, F., Rad, A.H.S., Sani, B. & Mozafari, H. (2021) Grain yield and qualitative of rapeseed genotypes change in response to exogenous application of salicylic acid and planting density. *Gesunde Pflanzen*, 73, 1–10.
- Garcion, C., Lohmann, A., Lamodièrre, E., Catinot, J., Buchala, A., Doermann, P. et al. (2008) Characterization and biological function of the ISOCHORISMATE SYNTHASE2 gene of *Arabidopsis*. *Plant Physiology*, 147, 1279–1287.
- Ghassemi-Golezani, K. & Farhangi-Abri, S. (2018) Changes in oil accumulation and fatty acid composition of soybean seeds under salt stress in response to salicylic acid and jasmonic acid. *Russian Journal of Plant Physiology*, 65, 229–236.
- Goffman, F.D., Alonso, A.P., Schwender, J., Shachar-Hill, Y. & Ohlrogge, J.B. (2005) Light enables a very high efficiency of carbon storage in developing embryos of rapeseed. *Plant Physiology*, 138, 2269–2279.
- Heneen, W.K., Geleta, M., Brismar, K., Xiong, Z., Pires, J.C., Hasterok, R. et al. (2012) Seed colour loci, homoeology and linkage groups of the C genome chromosomes revealed in *Brassica rapa*-*B. oleracea* monosomic alien addition lines. *Annals of Botany*, 109, 1227–1242.
- James, D.W., Jr., Lim, E., Keller, J., Plooy, I., Ralston, E. & Dooner, H.K. (1995) Directed tagging of the *Arabidopsis* FATTY ACID ELONGATION1 (FAE1) gene with the maize transposon activator. *The Plant Cell*, 7, 309–319.
- Kang, M., Abdelmageed, H., Lee, S., Reichert, A., Mysore, K.S. & Allen, R.D. (2013) AtMBP-1, an alternative translation product of LOS2, affects abscisic acid responses and is modulated by the E3 ubiquitin ligase AtSAP5. *The Plant Journal*, 76, 481–493.
- Kim, H.S. & Delaney, T.P. (2002) Over-expression of TGA5, which encodes a bZIP transcription factor that interacts with NIM1/NPR1, confers SAR-independent resistance in *Arabidopsis thaliana* to *Peronospora parasitica*. *The Plant Journal*, 32, 151–163.
- Kumar, N., Tokas, J., Raghavendra, M. & Singal, H.R. (2021) Impact of exogenous salicylic acid treatment on the cell wall metabolism and ripening process in postharvest tomato fruit stored at ambient temperature. *International Journal of Food Science & Technology*, 56, 2961–2972.
- Kunst, L., Taylor, D.C. & Underhill, E.W. (1992) Fatty acid elongation in developing seeds of *Arabidopsis thaliana*. *Plant Physiology and Biochemistry*, 30, 425–434.
- Lee, H., Guo, Y., Ohta, M., Xiong, L., Stevenson, B. & Zhu, J.K. (2002) LOS2, a genetic locus required for cold-responsive gene transcription encodes a bi-functional enolase. *The EMBO Journal*, 21, 2692–2702.
- Li, C., Qiu, J., Huang, S., Yin, J. & Yang, G. (2019) AaMYB3 interacts with AabHLH1 to regulate proanthocyanidin accumulation in *Anthurium andraeanum* (Hort.)—another strategy to modulate pigmentation. *Horticulture Research*, 6, 14.
- Li, Y., Beisson, F., Pollard, M. & Ohlrogge, J. (2006) Oil content of *Arabidopsis* seeds: the influence of seed anatomy, light and plant-to-plant variation. *Phytochemistry*, 67, 904–1015.
- Lian, J., Lu, X., Yin, N., Ma, L., Lu, J., Liu, X. et al. (2017) Silencing of BnTT1 family genes affects seed flavonoid biosynthesis and alters seed fatty acid composition in *Brassica napus*. *Plant Science*, 254, 32–47.
- Liu, W., Hildebrand, D.F. & Collins, G.B. (1995) Auxin-regulated changes of fatty acid content and composition in soybean zygotic embryo cotyledons. *Plant Science*, 106, 31–42.
- Liu, X., Lu, Y., Yuan, Y., Liu, S., Guan, C., Chen, S. et al. (2013) De novo transcriptome of *Brassica juncea* seed coat and identification of genes for the biosynthesis of flavonoids. *PLoS One*, 8, e71110.
- Liu, X., Yang, W., Mu, B., Li, S., Li, Y., Zhou, X. et al. (2018) Engineering of ‘Purple Embryo Maize’ with a multigene expression system derived from a bidirectional promoter and self-cleaving 2A peptides. *Plant Biotechnology Journal*, 16, 1107–1109.
- Liu, Z., Zhang, A., Zheng, L., Johnathan, A.F., Zhang, J. & Zhang, G. (2018) The biological significance and regulatory mechanism of c-Myc binding protein 1 (MBP-1). *International Journal of Molecular Sciences*, 19, 3868.
- Liu, Z., Zhang, Y., Ma, X., Ye, P., Gao, F., Li, X. et al. (2020) Biological functions of *Arabidopsis thaliana* MBP-1-like protein encoded by ENO2 in the response to drought and salt stresses. *Physiologia Plantarum*, 168, 660–674.
- Liu, Z., Zheng, L., Pu, L., Ma, X., Wang, X., Wu, Y. et al. (2020) ENO2 affects the seed size and weight by adjusting cytokinin content and forming ENO2-bZIP75 complex in *Arabidopsis thaliana*. *Frontiers in Plant Science*, 11, 574316.
- Lu, K., Wei, L., Li, X., Wang, Y. & Li, J. (2019) Whole-genome resequencing reveals *Brassica napus* origin and genetic loci involved in its improvement. *Nature Communications*, 10, 1154.
- Lv, Z., Guo, Z., Zhang, L., Zhang, F., Jiang, W., Shen, Q. et al. (2019) Interaction of bZIP transcription factor TGA6 with salicylic acid signaling modulates artemisinin biosynthesis in *Artemisia annua*. *Journal of Experimental Botany*, 70, 3969–3979.
- Martin, A.M., Martínez-Herrera, D., Cabrera-Poch, H.L. & Ponz, F. (1997) Variability in the interactions between *Arabidopsis thaliana* ecotypes and oilseed rape mosaic tobamovirus. *Australian Journal of Plant Physiology*, 24, 275–281.
- Meng, J., Shi, S., Gan, L., Li, Z. & Qu, X. (1998) The production of yellow-seeded *Brassica napus* (AACC) through crossing interspecific hybrids of *B. campestris* (AA) and *B. carinata* (BBCC) with *B. napus*. *Euphytica*, 103, 329–333.
- Mu, J., Tan, H., Zheng, Q., Fu, F., Liang, Y., Zhang, J. et al. (1998) LEAFY COTYLEDON1 is a key regulator of fatty acid biosynthesis in *Arabidopsis*. *Plant Physiology*, 148, 1042–1054.
- Namazkar, S., Stockmarr, A., Frenck, G., Egsgaard, H., Terkelsen, T., Mikkelsen, T. et al. (2016) Concurrent elevation of CO<sub>2</sub>, O<sub>3</sub> and temperature severely affects oil quality and quantity in rapeseed. *Journal of Experimental Botany*, 67, 4117–4125.
- Olsson, G. (1960) Species crosses within the genus *Brassica*. *Hereditas*, 46, 171–223.



- Prabhakar, V., Löttgert, T., Gigolashvili, T., Bell, K., Flügge, U.I. & Häusler, R.E. (2009) Molecular and functional characterization of the plastid-localized phosphoenolpyruvate enolase (ENO1) from *Arabidopsis thaliana*. *FEBS Letters*, 583, 983–991.
- Pu, G., Ma, D., Chen, J., Ma, L., Wang, H., Li, G. et al. (2009) Salicylic acid activates artemisinin biosynthesis in *Artemisia annua* L. *Plant Cell Reports*, 28, 1127–1135.
- Puttick, D., Dauk, M., Lozinsky, S. & Smith, M.A. (2009) Overexpression of a FAD3 desaturase increases synthesis of a polymethylene-interrupted dienoic fatty acid in seeds of *Arabidopsis thaliana* L. *Lipids*, 44, 753–757.
- Rogalski, M. & Carrer, H. (2011) Engineering plastid fatty acid biosynthesis to improve food quality and biofuel production in higher plants. *Plant Biotechnology Journal*, 9, 554–564.
- Shi, L., Tan, Y., Sun, Z., Ren, A., Zhu, J. & Zhao, M. (2019) Exogenous salicylic acid (SA) promotes the accumulation of biomass and flavonoid content in *Phellinus igniarius* (Agaricomycetes). *International Journal of Medicinal Mushrooms*, 21, 955–963.
- Sravankumar, T., Akash, Naik, N. & Kumar, R. (2018) A ripening-induced *SIGH3-2* gene regulates fruit ripening via adjusting auxin-ethylene levels in tomato (*Solanum lycopersicum* L.). *Plant Molecular Biology*, 98, 455–469.
- Srivastava, M.K. & Dwivedi, U.N. (2000) Delayed ripening of banana fruit by salicylic acid. *Plant Science*, 158, 87–96.
- Tang, Z., Li, J., Zhang, X., Chen, L. & Wang, R. (1997) Genetic variation of yellow-seeded rapeseed lines (*Brassica napus* L.) from different genetic sources. *Plant Breeding*, 116, 471–474.
- Thelen, J.J. & Ohlrogge, J.B. (2002) Both antisense and sense expression of biotin carboxyl carrier protein isoform 2 inactivates the plastid acetyl-coenzyme A carboxylase in *Arabidopsis thaliana*. *The Plant Journal*, 32, 419–431.
- Torrens-Spence, M.P., Bobokalonova, A., Carballo, V., Glinkerman, C.M., Pluskal, T., Shen, A. et al. (2019) PBS3 and EPS1 complete salicylic acid biosynthesis from isochorismate in *Arabidopsis*. *Molecular Plant*, 12, 1577–1586.
- Valero, D., Díaz-Mula, H.M., Zapata, P.J., Castillo, S., Guillén, F., Martínez-Romero, D. et al. (2011) Postharvest treatments with salicylic acid, acetylsalicylic acid or oxalic acid delayed ripening and enhanced bioactive compounds and antioxidant capacity in sweet cherry. *Journal of Agricultural and Food Chemistry*, 59, 5483–5489.
- Van der Does, D., Leon-Reyes, A., Koornneef, A., Van Verk, M.C., Rodenburg, N., Pauwels, L. et al. (2013) Salicylic acid suppresses jasmonic acid signaling downstream of SCFCO11-JAZ by targeting GCC promoter motifs via transcription factor ORA59. *The Plant Cell*, 25, 744–761.
- von Wettstein-Knowles, P., Olsen, J.G., McGuire, K.A. & Henriksen, A. (2006) Fatty acid synthesis. *The FEBS Journal*, 273, 695–710.
- Wang, H., Zhang, H., Yang, Y., Li, M., Zhang, Y., Liu, J. et al. (2020) The control of red colour by a family of MYB transcription factors in octoploid strawberry (*Fragaria × ananassa*) fruits. *Plant Biotechnology Journal*, 18, 1169–1184.
- Wang, J., Liu, Z., Liu, H., Peng, D., Zhang, J. & Chen, M. (2021) *Linum usitatissimum* FAD2A and FAD3A enhance seed polyunsaturated fatty acid accumulation and seedling cold tolerance in *Arabidopsis thaliana*. *Plant Science*, 311, 111014.
- Wang, Z., Chen, M., Chen, T., Xuan, L., Li, Z., Du, X. et al. (2014) *TRANS-PARENT TESTA2* regulates embryonic fatty acid biosynthesis by targeting *FUSCA3* during the early developmental stage of *Arabidopsis* seeds. *The Plant Journal*, 77, 757–769.
- Wei, X., Ju, Y., Ma, T., Zhang, J., Fang, Y. & Sun, X. (2020) New perspectives on the biosynthesis, transportation, astringency perception and detection methods of grape proanthocyanidins. *Critical Reviews in Food Science and Nutrition*, 3, 1–27.
- Wu, G. & Xue, H. (2010) *Arabidopsis*  $\beta$ -ketoacyl-[acyl carrier protein] synthase i is crucial for fatty acid synthesis and plays a role in chloroplast division and embryo development. *The Plant Cell*, 22, 3726–3744.
- Wu, P., Zhang, S., Zhang, L., Chen, Y., Li, M., Jiang, H. et al. (2010) Functional characterization of two microsomal fatty acid desaturases from *Jatropha curcas* L. *Journal of Plant Physiology*, 170, 1360–1366.
- Xu, H., Zou, Q., Yang, G., Jiang, S., Fang, H., Wang, Y. et al. (2020) MdMYB6 regulates anthocyanin formation in apple both through direct inhibition of the biosynthesis pathway and through substrate removal. *Horticulture Research*, 7, 72.
- Xu, L., Wu, J. & Zhao, Y. (2022) Salicylic acid-mediated diacylglycerol/triacylglycerol conversion affects the freezing tolerance of *Arabidopsis*. *Plant Growth Regulation*, 98, 1–10.
- Xu, W., Dubos, C. & Lepiniec, L. (2015) Transcriptional control of flavonoid biosynthesis by MYB-bHLH-WDR complexes. *Trends in Plant Science*, 20, 176–185.
- Xuan, L., Zhang, C., Yan, T., Wu, D., Hussain, N., Li, Z. et al. (2018) *TRANS-PARENT TESTA 4*-mediated flavonoids negatively affect embryonic fatty acid biosynthesis in *Arabidopsis*. *Plant, Cell & Environment*, 41, 2773–2790.
- Yilmaz, A., Rudolph, H.L., Hurst, J.J. & Wood, T.D. (2016) High-throughput metabolic profiling of soybean leaves by fourier transform ion cyclotron resonance mass spectrometry. *Analytical Chemistry*, 88, 1188–1194.
- Zander, M., La Camera, S., Lamotte, O., Métraux, J.P. & Gatz, C. (2010) *Arabidopsis thaliana* class-II TGA transcription factors are essential activators of jasmonic acid/ethylene-induced defense responses. *The Plant Journal*, 61, 200–210.
- Zhai, Y., Yu, K., Cai, S., Hu, L., Amoo, O., Xu, L. et al. (2019) Targeted mutagenesis of BnTT8 homologs controls yellow seed coat development for effective oil production in *Brassica napus* L. *Plant Biotechnology Journal*, 18, 1153–1168.
- Zhang, J., Liu, H., Sun, J., Li, B., Zhu, Q., Chen, S. et al. (2012) *Arabidopsis* fatty acid desaturase FAD2 is required for salt tolerance during seed germination and early seedling growth. *PLoS One*, 7, e30355.
- Zhong, C., Tang, Y., Pang, B., Li, X., Yang, Y., Deng, J. et al. (2020) The R2R3-MYB transcription factor GhMYB1a regulates flavonol and anthocyanin accumulation in *Gerbera hybrida*. *Horticulture Research*, 7, 78.
- Zhou, W., Chen, F., Zhao, S., Yang, C., Meng, Y., Shuai, H. et al. (2019) DA-6 promotes germination and seedling establishment from aged soybean seeds by mediating fatty acid metabolism and glycometabolism. *Journal of Experimental Botany*, 70, 101–114.

## SUPPORTING INFORMATION

Additional supporting information can be found online in the Supporting Information section at the end of this article.

**How to cite this article:** Liu, Z., Liu, H., Zheng, L., Xu, F., Wu, Y., Pu, L. et al. (2022) Enolase2 regulates seed fatty acid accumulation via mediating carbon partitioning in *Arabidopsis thaliana*. *Physiologia Plantarum*, 174(6), e13797. Available from: <https://doi.org/10.1111/ppl.13797>